

Effect of temperature on the optical properties of (InGa)(AsN)/GaAs single quantum wells

A. Polimeni^{a)} and M. Capizzi

Istituto Nazionale di Fisica della Materia, Dipartimento di Fisica, Università degli Studi di Roma "La Sapienza," Piazzale A. Moro 2, I-00185 Roma, Italy

M. Geddo

INFN-Udr Pavia, Via Bassi 6, I-27100 Pavia and Dipartimento di Fisica, Università di Parma, I-43100 Parma, Italy

M. Fischer, M. Reinhardt, and A. Forchel

Universität Würzburg, Technische Physik, Am Hubland 97074 Würzburg, Germany

(Received 13 March 2000; accepted for publication 6 September 2000)

$\text{In}_x\text{Ga}_{1-x}\text{As}_{1-y}\text{N}_y/\text{GaAs}$ single quantum wells emitting at room temperature in the wavelength range $\lambda=(1.3\text{--}1.55)\ \mu\text{m}$ have been studied by photoluminescence (PL). By increasing temperature, we find that samples containing nitrogen have a luminescence thermal stability and a room temperature emission efficiency higher than that of the corresponding N-free heterostructures. The temperature dependence of the PL line shape shows a progressive carrier detrapping from localized to extended states as T is increased. Finally, the extent of the thermal shift of the free exciton energy for different y indicates that the electron band edge has a localized character which increases with nitrogen content. © 2000 American Institute of Physics. [S0003-6951(00)00744-0]

There is growing interest in the optical^{1–14} and microscopic^{2,6,9,15} properties of (InGa)(AsN)/GaAs heterostructures, a feasible alternative to the (InGa)(AsP)/InP system for accessing the transmission windows of silica fibers.¹ This is possible thanks to the incorporation of a small amount of nitrogen in the (InGa)As matrix. In fact, a dramatic redshift of the alloy bandgap is commonly observed; about (60–100) meV per percent of N.^{2,5,6} The physical origin of such band-gap shrinkage has been investigated^{5,6} both experimentally and theoretically and modeled in terms of a N-induced interaction between conduction band states. Furthermore, the alloy disorder present in the $\text{In}_x\text{Ga}_{1-x}\text{As}_{1-y}\text{N}_y$ layers affects strongly the carrier motion and leads to a radiative recombination generally dominated by localized excitons.^{6–8,12,13}

In this letter, we report on the effect of temperature, T , on the photoluminescence (PL) properties of $\text{In}_x\text{Ga}_{1-x}\text{As}_{1-y}\text{N}_y/\text{GaAs}$ single quantum wells (QWs). First, the luminescence signal of QWs containing N shows a stronger thermal stability with respect to that of N-free QWs. At room temperature, the emission efficiency in “nitrogenated” samples is higher than in the corresponding samples without N. Second, in samples containing nitrogen for increasing T we observe a smooth decrease in the population ratio between localized (LE) and free excitons (FE), the latter being dominant at room temperature. Finally, a reduced thermal redshift of the FE energy between $T=10\ \text{K}$ and room temperature is observed when y increases. We interpret our results in terms of an enhanced localized character of the electron wavefunction for larger nitrogen content.

Three $\text{In}_x\text{Ga}_{1-x}\text{As}_{1-y}\text{N}_y/\text{GaAs}$ single QWs grown by solid source molecular beam epitaxy (MBE) have been

investigated: AN ($x=0.25, y=0.005$), BN ($x=0.32, y=0.015$), and CN ($x=0.38, y=0.022$). All samples, including three N-free blanks (A, B, and C) with the same x , are $6.5\pm 0.5\ \text{nm}$ thick. N_2 cracking was obtained by using an electron cyclotron resonance plasma source separated from the main MBE chamber. This arrangement prevents N incorporation in the GaAs barriers thus leading to very well defined heterointerfaces. PL, excited by the 515 nm line of an Ar^+ laser, was dispersed by a double 3/8 m or a single 1 m monochromator and detected by an (InGa)As photodiode or a cooled avalanche Ge detector.

The room temperature (RT) PL spectra of all samples are shown in Fig. 1 for a same level of excitation. The large redshift of the PL peak position in the “nitrogenated” QWs has allowed us to reach the wavelength range (1.3–1.55) μm of interest for data transmission through optical fibers. This has led to the first continuous wave operation of GaAs based 1.3 μm distributed feedback laser diodes with a single $\text{In}_x\text{Ga}_{1-x}\text{As}_{1-y}\text{N}_y$ QW as active medium.¹⁷ Unlike in earlier PL works,^{1,2,9} the PL integrated intensity of “nitrogenated” samples is greater than that of the corresponding N-free blanks at RT and is lower, instead, at $T=10\ \text{K}$; see the inset of Fig. 1 for samples C and CN. Therefore, although N introduces nonradiative recombination centers, the larger carrier confinement achieved in our QWs with nitrogen makes the luminescence signal more thermally stable, enough to compensate the effect of these nonradiative centers. Post-growth annealing treatments do not influence the PL efficiency.

Figures 2(a) and 2(b) show PL spectra at different T 's for samples BN and CN, respectively; sample AN (not shown) behaves as sample BN. At $T=10\ \text{K}$ the spectra are due to a single recombination, LE. For $T>50\ \text{K}$ (AN and BN) and for $T>160\ \text{K}$ (CN), a new band, FE, appears at an energy higher than the LE band and dominates the spectrum

^{a)}Electronic mail: polimeni@roma1.infn.it

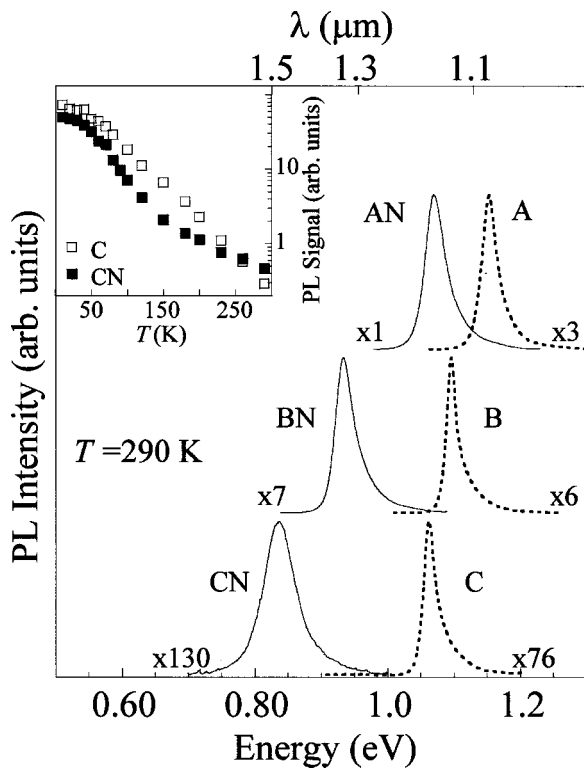


FIG. 1. Peak normalized room temperature photoluminescence, PL, spectra of samples with (continuous line) and without (dashed line) nitrogen, taken at laser power $P=60 \text{ W/cm}^2$. Normalization factors are given for each spectrum. Sample properties are A: $x=0.25, y=0$; AN: $x=0.25, y=0.005$; B: $x=0.32, y=0$; BN: $x=0.32, y=0.015$; C: $x=0.38, y=0$; CN: $x=0.38, y=0.022$. The inset shows the PL integrated intensity vs temperature in samples C and CN.

up to RT without any remarkable line shape change. The intensity of this FE band increases with respect to that of the LE band for increasing excitation power density. We at-

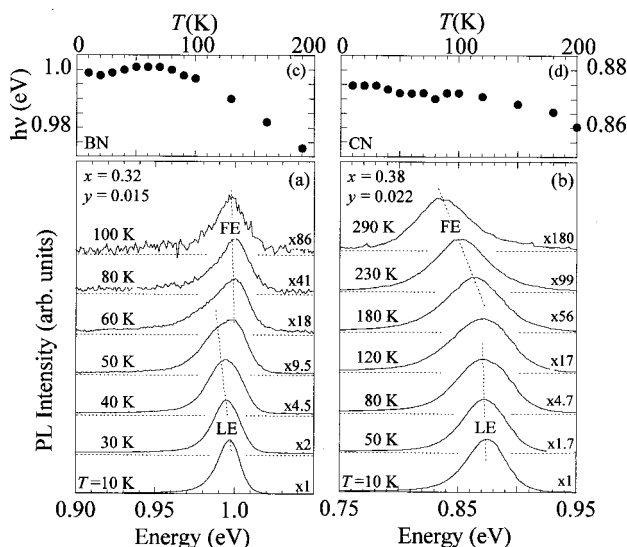


FIG. 2. (a) Peak normalized photoluminescence, PL, spectra of sample BN for different temperatures (laser power, $P=8 \text{ W/cm}^2$). LE and FE indicate recombination from localized and free excitons, respectively. (b) The same as in (a) for sample CN ($P=18 \text{ W/cm}^2$), where LE and FE recombinations are not well resolved. Normalization factors are given for each spectrum. (c) Temperature dependence of the peak energy, $h\nu$, of PL for sample BN. (d) Same as in (c) for sample CN.

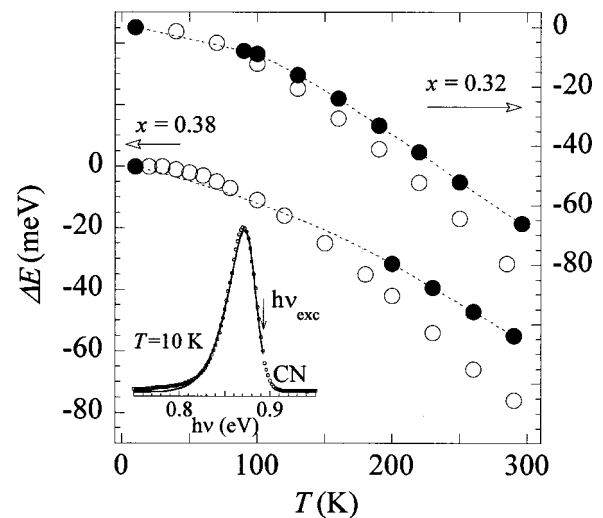


FIG. 3. Dependence on T of the free exciton photoluminescence energy, ΔE , measured with respect to the value at $T=10 \text{ K}$ for samples B ($x=0.32, y=0.015$) and C ($x=0.38, y=0.022$) (open dots) and BN ($x=0.32, y=0.015$) and CN ($x=0.38, y=0.022$) (full dots). Dotted lines are guides to the eye. Inset: low- T (laser power, $P=0.8 \text{ W/cm}^2$) PL spectrum of sample CN (open circles). The continuous line is a simulation to the data, as discussed in the text. $h\nu_{\text{exc}}$ indicates the free exciton energy.

tribute the LE and FE bands to localized and free exciton recombination, respectively.

The PL peak energy, $h\nu$, is shown as a function of T in Figs. 2(c) and 2(d) for samples BN and CN, respectively. With increasing T , $h\nu$ shows a nonmonotonous behavior in sample BN and is nearly constant in sample CN, which suggests a carrier redistribution between localized and extended states of the well. In particular, in sample CN (having the higher nitrogen content) carrier freezeout in local energy minima persists up to $T=200 \text{ K}$ and may affect device performances even at high T 's. Moreover, at low T all nitrogenated QWs exhibit asymmetric PL bands characterized by a low-energy tail, as shown in Fig. 2 and in the inset of Fig. 3 for sample CN, which is absent in the N-free samples. This tail is present in other (InGa)(AsN) QWs and epilayers^{2,6-8,10,13,18} and in a large number of semiconductor alloys.^{19,20} In order to determine the actual FE recombination energy at low T and explain the $T=10 \text{ K}$ PL line shape, a suitable line shape analysis has been introduced. The low energy tail can be accounted for by alloy fluctuations¹⁹ which give rise to an exponential density of localized states²¹⁻²³

$$g(h\nu) = g_0 \exp\left\{-\left[\frac{h\nu - h\nu_{\text{exc}}}{\varepsilon_0}\right]^{3/2}\right\}, \quad (1)$$

where $h\nu_{\text{exc}}$ is the FE energy, ε_0 is a characteristic energy, and g_0 is a constant. The PL spectrum is then given by^{19,20}

$$L(h\nu) \propto g(h\nu) \tau(h\nu) \exp[f(h\nu)]. \quad (2)$$

$\tau(h\nu)$ is the exciton radiative lifetime and $\tau^{-1}(h\nu) \propto 1 + \exp\{\delta[\varepsilon_M - (h\nu_{\text{exc}} - h\nu)]\}$, with δ the inverse of an effective temperature and ε_M the energy at which the radiative recombination probability equals the transfer probability toward deeper states.²³ For $\varepsilon < \varepsilon_M$, localized excitons recombine radiatively, while, for $\varepsilon > \varepsilon_M$, excitons relax to lower energy states $\varepsilon' < \varepsilon$. Finally, $f(h\nu; \varepsilon_0, h\nu_{\text{exc}}, \delta, \varepsilon_M)$ is a function whose expression can be found in Ref. 19.

The full line in the inset of Fig. 3 is a simulation of the PL spectrum using $L(h\nu)$ for sample CN, with $\delta = 0.15 \text{ meV}^{-1}$, $h\nu_{\text{exc}} = 0.892 \text{ eV}$, $\varepsilon_0 = 34 \text{ meV}$, and $\varepsilon_M = 0.882 \text{ eV}$. The last value for ε_M is 10 meV lower than $h\nu_{\text{exc}}$, close to that found from time-resolved PL in a $\text{In}_{0.03}\text{Ga}_{0.97}\text{As}_{0.99}\text{N}_{0.01}$ epilayer.¹⁷ We suggest that the microscopic origin of the low-energy tail is related to In–N clusters whose composition (and energy distribution) is given by the Poisson law. At low T , carriers occupy preferentially these states, while, at high T , they are thermally activated toward the higher FE energy states (see Fig. 2). Also, the T value at which localized excitons begin to be ionized increases with y thus indicating that the number and/or potential depth of the carrier trapping centers is proportional to the N concentration.

Figure 3 shows the dependence on T of the FE energy, ΔE , measured with respect to the value at $T = 10 \text{ K}$ for samples with (full dots) and without (open dots) nitrogen. For samples containing nitrogen the FE energy at $T = 10 \text{ K}$ has been obtained from the simulation described above. For increasing T , ΔE in sample BN is roughly the same as in sample B up to $T \sim 100 \text{ K}$, then it slows down with an overall effective band-gap reduction from $T = 10$ to $T = 295 \text{ K}$ which is 19% smaller with respect to the N-free QW. This behavior is more pronounced in sample CN which has a higher N content, where the reduction in ΔE measured respect to sample C is 32%. To further support the results shown in Fig. 3, we carried out photoreflectance (PR) measurements between $T = 90 \text{ K}$ and ambient temperature. PR data display a behavior analogous to that of PL data in terms of the differences in the thermal band-gap shrinkage between samples with and without nitrogen. Recently, effects similar to those reported here were observed in Ga(AsN) epilayers by T dependent absorption measurements,¹⁴ while a different behavior was observed for PR measurements in (InGa)(AsN)/GaAs QWs.¹² The large “optical bowing” observed in (InGa)As alloys upon incorporation of very small amount of N has been attributed to an anticrossing between the conduction band (CB), states and a localized level introduced by nitrogen.⁵ A similar model could explain the temperature dependence of the FE band reported here if one assumes that the N-related localized level has an absolute energy, which does not vary much with T , as observed in the case of carriers localized on a deep center.^{24,25} Finally, pseudopotential supercell calculations in $\text{GaAs}_{1-x}\text{N}_x$ alloys show that N incorporation leads to an interaction of Γ and L states that affects the energy position of the lowest CB minimum at ambient pressure.¹⁶

In this framework, the extent of band mixing increases with y and results in an enhanced localized character of the conduction band edge in real space and in an increase of the effective mass, also reported.²⁶ All these models suggest that, for increasing y the electronic energy levels might depend less on temperature, as found here.

In conclusion, we have grown $\text{In}_x\text{Ga}_{1-x}\text{As}_{1-y}\text{N}_y$ single quantum wells which emit at room temperature in the energy range of interest for telecommunications. The PL efficiency of “nitrogenated” QWs at RT is larger than that of the corresponding twin samples without nitrogen. The dependence on temperature of the PL spectra indicates the presence of localized and free carriers which dominate the radiative recombination processes at low and high T , respectively. It also suggests that nitrogen in $\text{In}_x\text{Ga}_{1-x}\text{As}$ behaves as a deep level interacting with the electron extended states of the host material, in agreement with theoretical models recently proposed.

The authors thank F. Martelli for helpful discussions and A. Miriametro for technical assistance.

- ¹M. Kondow, K. Uomi, A. Niwa, T. Kitatani, S. Watahiki, and Y. Yazawa, *Jpn. J. Appl. Phys.*, Part 1 **35**, 1273 (1996).
- ²H. P. Xin and C. W. Tu, *Appl. Phys. Lett.* **72**, 2442 (1998).
- ³P. Perlin, S. Subramanya, D. E. Mars, J. Kruger, N. A. Shapiro, H. Siegle, and E. R. Weber, *Appl. Phys. Lett.* **73**, 3703 (1998).
- ⁴S. R. Kurtz, A. A. Allerman, E. D. Jones, J. M. Gee, J. J. Banas, and B. Hammons, *Appl. Phys. Lett.* **74**, 729 (1999).
- ⁵W. Shan, W. Walukiewicz, J. W. Ager III, E. E. Haller, J. F. Geisz, D. J. Friedman, J. M. Olson, and S. R. Kurtz, *Phys. Rev. Lett.* **82**, 1221 (1999).
- ⁶H. P. Xin, K. L. Kavanagh, Z. Q. Zhu, and C. W. Tu, *Appl. Phys. Lett.* **74**, 2337 (1999).
- ⁷R. A. Mair, J. Y. Lin, H. X. Jiang, E. D. Jones, A. A. Allerman, and S. R. Kurtz, *Appl. Phys. Lett.* **76**, 188 (1999).
- ⁸I. A. Buyanova, W. M. Chen, G. Pozina, J. P. Bergman, B. Monemar, H. P. Xin, and C. W. Tu, *Appl. Phys. Lett.* **75**, 501 (1999).
- ⁹M. Sopanen, H. P. Xin, and C. W. Tu, *Appl. Phys. Lett.* **76**, 994 (2000).
- ¹⁰M. Hetterich, M. D. Dawson, A. Yu. Egorov, D. Bernklau, and H. Riechert, *Appl. Phys. Lett.* **76**, 1030 (2000).
- ¹¹E. D. Jones, N. A. Modine, A. A. Allerman, S. R. Kurtz, A. F. Wright, S. T. Tozer, and X. Wei, *Phys. Rev. B* **60**, 4430 (1999).
- ¹²L. Grenouillet, C. Bru-Chevallier, G. Guillot, P. Gilet, P. Duvaut, C. Vanuffel, A. Million, and A. Chevanes-Paule, *Appl. Phys. Lett.* **76**, 2241 (2000).
- ¹³S. Francoeur, S. A. Nikishin, C. Jin, Y. Qiu, and H. Temkin, *Appl. Phys. Lett.* **75**, 1538 (1999).
- ¹⁴K. Uesugi, I. Suemune, T. Hasegawa, T. Akutagawa, and T. Nakamura, *Appl. Phys. Lett.* **76**, 1285 (2000).
- ¹⁵Y. L. Soo, S. Huang, Y. H. Kao, J. G. Chen, S. L. Hulbert, J. F. Geisz, S. Kurtz, J. M. Olson, S. R. Kurtz, E. D. Jones, and A. A. Allerman, *Phys. Rev. B* **60**, 13605 (1999).
- ¹⁶T. Mattila, S. H. Wei, and A. Zunger, *Phys. Rev. B* **60**, R11245 (1999).
- ¹⁷M. Reinhardt, M. Fischer, J. Hofmann, M. Kamp, and A. Forchel, *IEEE Photonics Technol. Lett.* **12** (2000).
- ¹⁸M. R. Gokhale, J. Wei, H. Wang, and S. R. Forrest, *Appl. Phys. Lett.* **74**, 1287 (1999).
- ¹⁹D. Ouadjaout and Y. Marfaing, *Phys. Rev. B* **41**, 12096 (1990).
- ²⁰A. Ait-Ouali, R.-F. Yip, J. L. Brebner, and R. A. Masut, *J. Appl. Phys.* **83**, 3153 (1998).
- ²¹B. Halperin and M. Lax, *Phys. Rev.* **148**, 722 (1996).
- ²²E. Cohen and M. D. Sturge, *Phys. Rev. B* **25**, 3828 (1982).
- ²³M. Oueslati, C. Benoit à la Guillaume, and M. Zouaghi, *Phys. Rev. B* **37**, 3037 (1988).
- ²⁴P. W. Yu, *Phys. Rev. B* **42**, 11889 (1990).
- ²⁵J. Liang, J. Zhao, and Y. Gao, *J. Lumin.* **63**, 41 (1995).
- ²⁶C. Skierbiszewski, P. Perlin, P. Wisniewski, W. Knap, T. Suski, W. Walukiewicz, W. Shan, K. M. Yu, J. W. Ager, E. E. Haller, J. F. Geisz, and J. M. Olson, *Appl. Phys. Lett.* **76**, 2409 (2000).